

RELAZIONE SCIENTIFICA
SHORT-TERM MOBILITY Anno 2015

Fruitore

MARIAROSARIA CALVELLO

*ISTITUTO DI METODOLOGIE PER L'ANALISI AMBIENTALE (IMAA),
CONSIGLIO NAZIONALE DELLE RICERCHE*

Dip. SCIENZE DEL SISTEMA TERRA E TECNOLOGIE PER L'AMBIENTE

Titolo del programma di ricerca:

**Studio dell'influenza delle componenti degli aerosol atmosferici al suolo su
quelle colonnari con un focus sulla componente carboniosa**

Periodo di riferimento

23/09/2015 - 16/10/2015

Istituto ospitante

**INSTITUTE OF EARTH ENVIRONMENT (IEE), CHINESE ACADEMY OF
SCIENCES (CAS)**

Introduction

Atmospheric aerosols play a fundamental role in atmospheric processes significantly impacting environment, health and climate. Strong uncertainties in aerosol properties retrieval are still present pushing the scientific community to improve and intensify in situ observations together with remote sensing of aerosols and the use of models (Calvello et al., 2010; Sinha et al., 2013; Latha et al., 2014; van Beelen et al., 2014; Perrone et al., 2015). An extended coverage for integrated aerosol observations is needed especially for areas where, in recent years, the rapid economic growth has led to a drastic change in aerosol loading and characteristics. As an example, during last years, China has been making relevant efforts to assess aerosol properties over areas as large as possible trying to obtain a better knowledge on their role on climate and human health (Huang et al., 2014; Cui et al, 2015, Rohde and Muller 2015).

The aim of the present research program was to investigate the possible integration of ground-based radiometric and in-situ measurements collected at the urban Chinese site of Xi'an by the integration of radiometric measurements, chemical measurements and the use of a model. Columnar radiometric data, in fact, can be used as an input for a suitable model to infer aerosol composition to be compared to in-situ data. The model considered here is based on the use of OPAC (Optical Properties of Aerosol and Clouds by Hess et al. (1998)) aerosol types, as firstly proposed by Satheesh and Srinivasan (2005). The technique was recently tested on a series of AOD datasets obtained in different sites and loading conditions in Italy (Esposito et al., 2014; Pavese et al., 2014), allowing the identification of the main columnar components of atmospheric aerosols. In some cases, a comparison with in-situ data was obtained, showing interesting results as for example the significant presence of black carbon in air masses coming from Saharan desert, revealed both over the column and at the ground level.

The possibility to apply the above-mentioned technique to the Cimel radiometric data available at the Institute of Earth Environment, Chinese Academy of Sciences (IEECAS hereafter), represented an useful opportunity to test the model in conditions of heavy pollution and to gather more information on aerosol columnar composition. The comparison among model results and in-situ data available at IEECAS, allowed to assess if and in what conditions, aerosol columnar properties are influenced by those at the ground level.

The present report describes the research activities carried out during the Short Term Mobility (STM) period at the IEECAS in Xi'an. In the first section, an overview of the site peculiarities and

of the IEECAS experimental facilities and data made available by the hosting research group dataset is given, then, methods used for data analysis and main obtained results were described in section 4 and 5, respectively.

1. The Xi'an urban site and the IEECAS experimental facilities

Xi'an is one of the largest northern Chinese cities with a growing population of 8.4 million in 2010 (Hu, 2012). The city is located 400 m above sea level on the agriculturally-productive Guanzhong Plain, at the south edge of the Loess Plateau which represents an important dust source for the site (Cao et al., 2005, Cao et al., 2009). Figure 1 shows the city location in China.



Figure 1. Xi'an location. Aerial photography courtesy of Google Earth (<http://earth.google.com/>).

Xi'an is an inland developing city that experiences high level of pollution mainly due to residential coal combustion emissions, especially from November to February, and to traffic, with a number of vehicles that has increased from approximately half a million in 2006 to more than 1.3 million in 2010 (Hu, 2012).

Another relevant source of pollution is represented by biomass burning associated to agricultural activities in the Guanzhong Plain, which is a base for food production in China (Cao et al., 2015). This results in elevated carbonaceous aerosol loadings over the entire year contributing to the high PM levels in Xi'an (Cao et al., 2005). A study from Cao et al., 2007 revealed that, among 14 cities in China, the highest emissions of carbonaceous aerosols were measured in Xi'an. Another important contribution to the pollution at the site comes from the three major soluble inorganic species (sulfate, nitrate and ammonium) accounting for 32.4% of the PM_{2.5} mass (Zhang et al., 2011) associated to traffic, heating and industrial emissions. In general the abundance of fine particles, mainly < 1.0 μm in size, characterizes aerosol number size distributions at Xi'an as

recently assessed by Hu et al., 2012 who analyzed a dataset of Scanning Electron Microscope (SEM) samplings.

Finally a not negligible contribution from locally produced dust particles has to be taken into account due to fugitive dust, both from traffic and from the many construction sites all over the city.

For the analysis carried out in the framework of the STM research program, aerosol data, made available by the hosting research group guided by Prof. Junjii Cao, have been collected at the IEECAS monitoring site (34.22°N, 108.87°E; 389 m a.s.l) located in a developing residential area about 15 km south of downtown Xi'an.

In particular, radiometric data have been obtained by means of a Cimel CE318-NE type sun-sky radiometer (Cimel Electronique, Paris, France) installed on the roof of the main building of the IEECAS with a time resolution of 15 minutes, at the nine wavelengths of 340, 380, 440, 500, 675, 870, 940, 1020 and 1640 nm. Further details about the columnar aerosol optical measurements can be found in Su et al., 2014.

Chemical in-situ data used in the present study have been obtained by different measurement techniques with a 24-h temporal resolution (Cao et al., 2005; Shen et al., 2011; Zhang et al., 2011):

- Elemental Carbon (EC) and Organic Carbon (OC) content were derived by means of the Desert Research Institute (DRI) Model 2001 Thermal/Optical Carbon Analyzer (Atmoslytic Inc., Calabasas, CA, USA) following the IMPROVE (Interagency Monitoring of Protected Visual Environments) thermal/optical reflectance (TOR) protocol;
- ion chromatography (IC; Dionex 500, Dionex Corp., Sunnyvale, CA) was used to determine the concentrations of three anions (Cl^- , NO_3^- and SO_4^{2-}) and two cations (Na^+ , NH_4^+) in aqueous extracts of sampled filters;
- Al, Si, Ca, Ti and Fe concentrations were measured by energy-dispersive X-ray fluorescence (ED-XRF) spectrometry.

2. Methods

The first phase of the STM research activity was devoted to test the radiometric aerosol model on columnar CIMEL measurements collected at IECAAS in order to obtain columnar composition from measured AODs. The model follows the assumption proposed by Hess, 1998 (Hess, 1998) of considering the atmospheric aerosol as constituted by different components characterized by different size distributions and refractive indices.

In particular the nine components considered for the present study were: Water Soluble (WS), Soot (BC), Sea Salt accumulation (SSacc), Sea Salt coarse (SScoa), Mineral transported (MT),

Mineral nucleation (*Mnucl*), Mineral accumulation (*Macc*), Mineral coarse (*Mcoa*), and Insoluble (*Ins*). Each aerosol component was assumed to have a log-normal size distribution with a fixed mean radius and mode width as reported in Table 1 together with real and imaginary parts of refractive indices.

Table 1. Mean radius, mode width and refraction index describing the nine aerosol components

| Aerosol component | r (μm) | σ | Real refr. index | Imaginary refr. index |
|---|--------|------|------------------|-----------------------|
| Water soluble (<i>WS</i>) | 0.029 | 2.24 | 1.44 | -0.00265 |
| Soot (<i>BC</i>) | 0.018 | 2.0 | 1.75 | -0.45 |
| Sea salt-accumulation mode (<i>SSacc</i>) | 0.378 | 2.03 | 1.38 | -4.5 10 ⁻⁹ |
| Sea salt (coarse mode) (<i>SScoa</i>) | 3.17 | 2.03 | 1.38 | -4.5 10 ⁻⁹ |
| Mineral transported (<i>MT</i>) | 0.50 | 2.2 | 1.53 | -0.0078 |
| Mineral nucleation (<i>Mnucl</i>) | 0.07 | 1.95 | 1.53 | -0.0078 |
| Mineral accumulation (<i>Macc</i>) | 0.39 | 2.0 | 1.53 | -0.0078 |
| Mineral coarse (<i>Mcoa</i>) | 1.90 | 2.15 | 1.53 | -0.0078 |
| Insoluble (<i>Ins</i>) | 0.471 | 2.51 | 1.53 | -0.0078 |

Aerosol Optical Depths were computed by the model according to the Mie theory:

$$\tau_{\lambda_i}^{comp} = \tau_i^{comp} = \sum_{j=1}^k \int_0^{\infty} \pi r^2 Q_{extj}(m_j, r, \lambda_i) S_j n_j(r) dr, \quad (1)$$

where Q_{extj} is the extinction coefficient, m_j is the complex refractive index and S_j is the scaling factor for the j -th aerosol component which represents the contribution of each aerosol component to the total columnar AOD. S_j were calculated by means of a least-square technique applied to the radiometric measurements over the spectral range minimizing the following quantity: (Satheesh and Srinivasan, 2005):

$$\chi^2 = \sum_{i=1}^N \frac{(\tau_i^{meas} - \tau_i^{comp})^2}{(\Delta \tau_i^{meas})^2}, \quad (2)$$

where τ_i^{meas} are the measured optical depths, τ_i^{comp} are the computed optical depths, and $\Delta\tau_i^{\text{meas}}$ is the experimental error.

In a second phase of the research activity the model results were compared to in-situ chemical data collected at the same site of CIMEL ones.

3. Discussion and results

In order to test the model, a first set of radiometric data, collected on November 2012 (from 2nd to 6th and on 13th and 16th), was chosen among those previously analyzed in the work by Su et al., 2014. As reported in Su et al., 2014 on November 2nd a strong pollution event was detected at Xi'an site followed by the advection of dust on November 3rd corresponding to an abrupt change in aerosol optical properties. The application of the model to this study case was thought to be suitable to verify if it could well represent the changes in aerosol properties.

For an overview of the dataset, Cimel measurements days, number of measurements per day, daily mean AOD@500 and alpha values with corresponding standard deviations are reported in Table 2.

Table 2. Cimel measurements days, number of measurements per day, daily mean AOD@500 and alpha values with corresponding standard deviations for the period 2 -16 November 2012.

| | Number of measurements | AOD @ 500 Daily mean \pm St.Dev | Alpha Daily mean \pm St.Dev |
|------------------|-------------------------------|---|---|
| 2 nov 12 | 26 | 0.87 \pm 0.06 | 1.31 \pm 0.04 |
| 3 nov 12 | 26 | 0.5 \pm 0.1 | 0.13 \pm 0.03 |
| 4 nov 12 | 46 | 0.26 \pm 0.05 | 0.56 \pm 0.06 |
| 5 nov 12 | 34 | 0.5 \pm 0.1 | 1.02 \pm 0.08 |
| 6 nov 12 | 11 | 0.9 \pm 0.1 | 1.22 \pm 0.04 |
| 13 nov 12 | 15 | 0.35 \pm 0.03 | 0.90 \pm 0.03 |
| 16 nov 12 | 4 | 0.42 \pm 0.07 | 0.46 \pm 0.04 |

A first try of model application was made by using only five of the nine components of Table 1, as usually did for the Italian sites, where a zero contribution was generally obtained for *Mnucl*, *Macc*, *Mcoa* and *Ins* components. Then, as a further step, due to the Xi'an site peculiarities especially related to fugitive dust, the model was run using all the nine components that accounted for different dust modes. As a result, we found a contribution from all the nine components even if sea salts particles seemed to have a minor impact on the ADOs, as expected for an inland site as Xi'an. Anyway we decided to use all the nine components for the subsequent analysis.

In Figure 1 a-b, daily mean values of the model-estimated AOD@500 for each component together with total AOD@500 are reported for the considered days. As a reference, daily averaged measured AOD@500 and Ångström parameter alpha are shown in Figure 1 c-d.

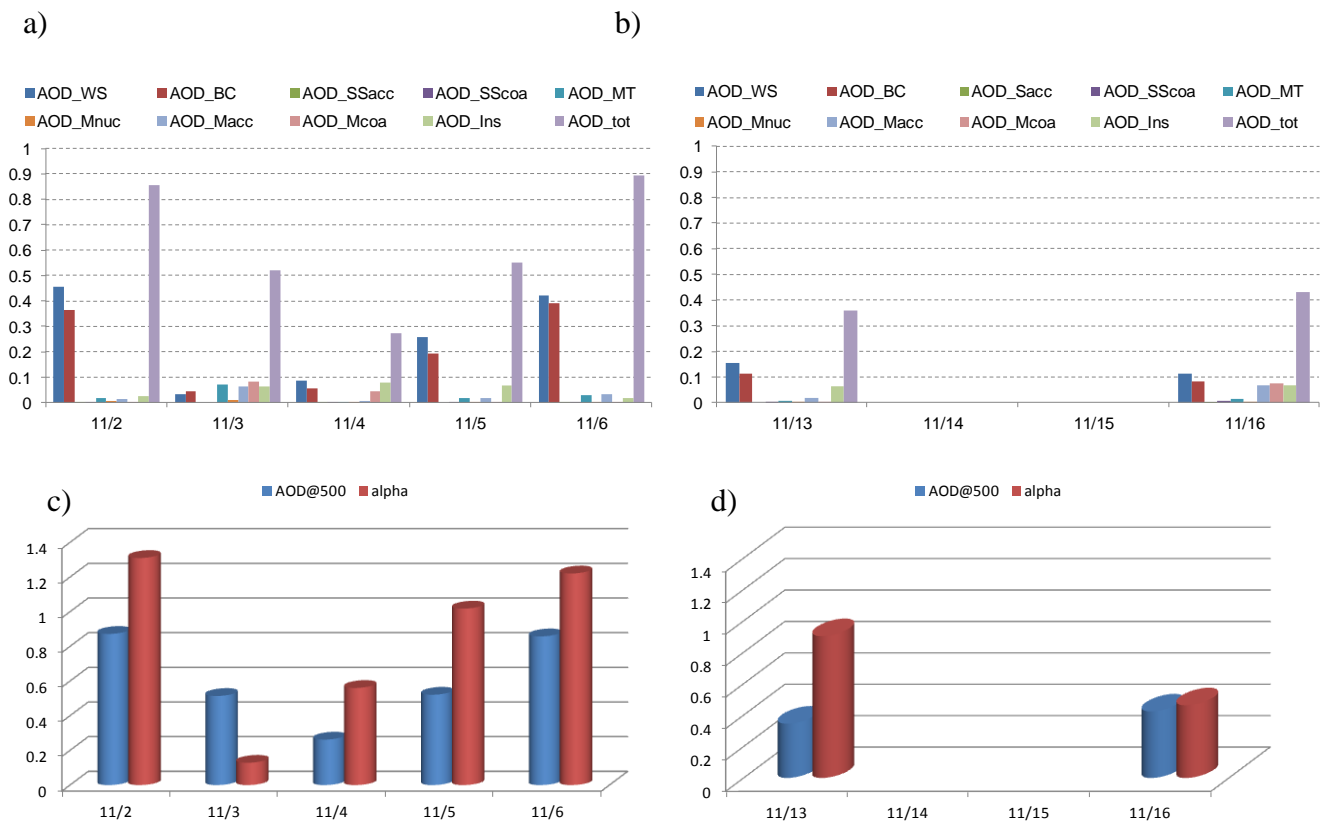


Figure 1. Daily mean values of the model-estimated AOD@500 for each component together with total AOD@500 for 2-6 November (a), and 13 and 16 November (b). Daily averaged measured AOD@ 500 and alpha parameter for 2-6 November (c), and 13 and 16 November (d).

As it is possible to see, the model was able to follow the variations in aerosol columnar composition from November 2nd, when the city experienced an intense pollution episode, to November 3rd when dust advection dominates aerosol loading at the site. In the first case the main components were *WS* and *BC* indicating a predominance of fine aerosols. On November 3rd, all the four dust components

were represented. Looking at the other days, higher total aerosol values corresponded to a dominance of *WS* and *BC* components.

Percentage contributions of the different components to the total AOD@500 are reported in Figure 2. As already mentioned, apart from November 3rd, *WS* and *BC* components dominated the aerosol loading at the site with percentages varying from a minimum value of 45% on November 16th, to a maximum of 96% on November 2nd. Sea salt particles represented a not negligible contribution only on November 3rd when they accounted for the 28% of the total AOD@500 probably due to the passage of transported air-masses (Su et al., 2014). Among dust components, *MT* and *Macc* were always present even if in small percentages going from 3% on November 4th to 28% on November 3rd for their sum. When present, *Mcoa* component gave a relevant contribution of 16% on November 3rd and November 4th, and 18% on November 16th. Also the *Ins* component was always present with percentages varying from the minimum percentage of 2% on November 6th to the maximum percentage of 29% on November 4th.

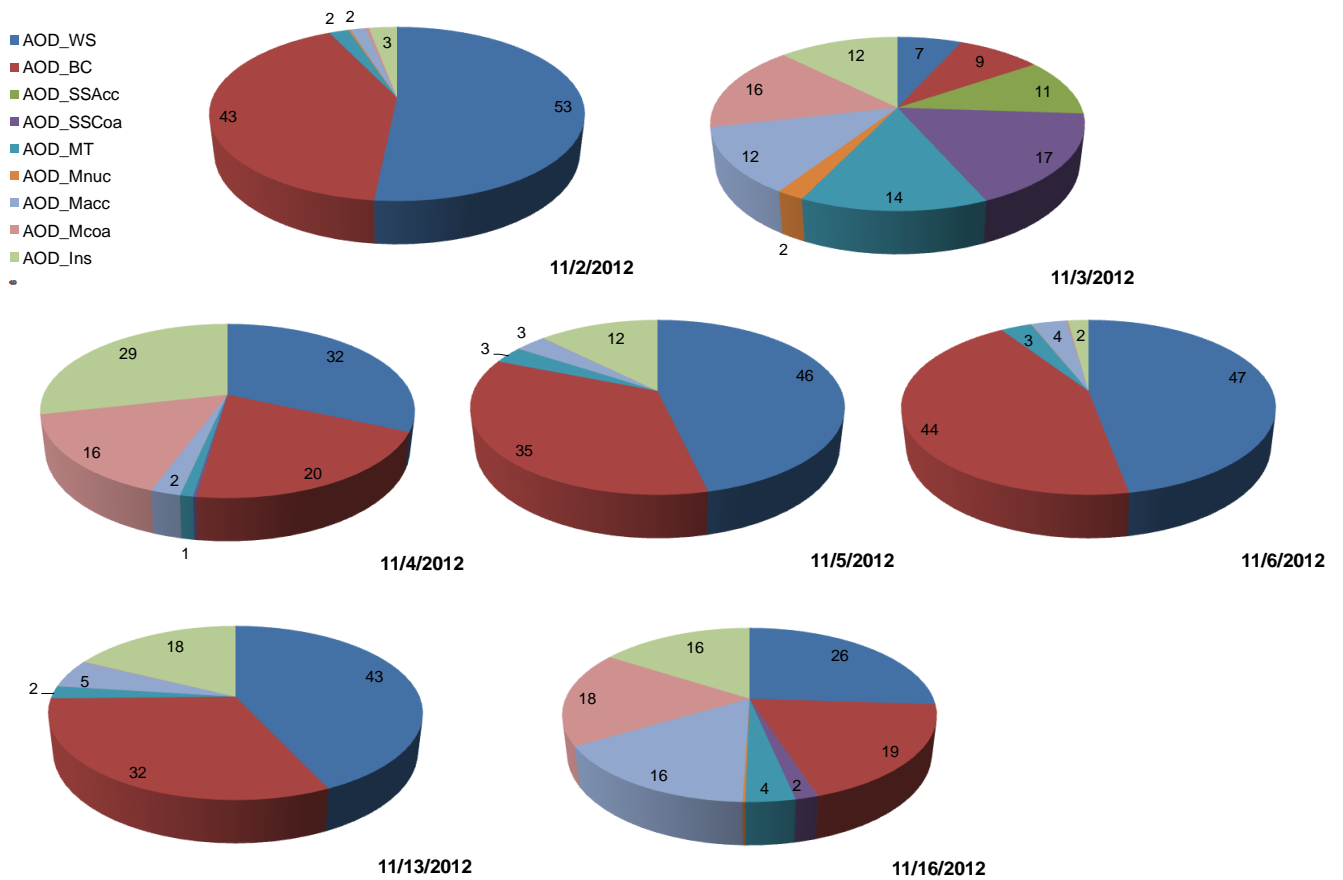


Figure 2. Percentage contributions of the different components to the total AOD@500 for 2-6 and 13, 16 November 2012.

3.1 Comparison with in-situ data

Model results related to the short period considered were compared to in situ chemical data. To this aim 24-h averaged radiometric data were taken into account.

Similar trends were observed for the modeled *WS* component of AOD@500 and the water soluble fraction calculated as the linear combination of NO_3^- and SO_4^{2-} concentrations measured at ground (Figure 3a). Figure 3b shows the good agreement found between *WS* component and NH_4^+ concentration temporal trends. The calculated values of correlation coefficients were $R^2 = 0.9$ and $R^2 = 0.7$ respectively. On the contrary, dissimilar trends and negligible correlations were found when comparing the modeled *BC* component of AOD@500 to both EC and OC concentrations measured at ground.

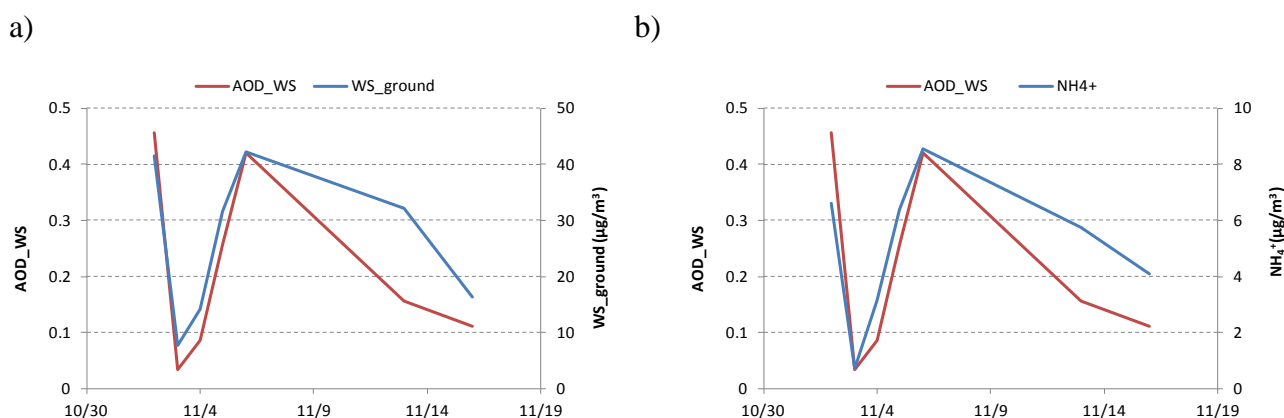


Figure 3. Temporal trends of daily mean *WS* modeled component of AOD@500 and (a) water soluble fraction measured at ground; (b) NH_4^+ cation measured at ground for 2-6 and 13, 16 November 2012.

One possible explanation could be related to the different sampling time of the two measurements because radiometric ones, carried out only during sunny hours, started after and stopped before the two typical diurnal *BC* peaks associated to traffic (Cao et al., 2009) probably missing the more intense *BC* emissions. Moreover the additional source of carbonaceous aerosols associated to residential heating, certainly present in these November measurements, gave a relevant contribution from late afternoon on (Cao et al., 2009), when radiometer was not measuring. This did not happen for water vapor fraction whose maximum concentrations are usually found in the central hours of the day (Shon et al., 2013).

If one excludes the day of November 3rd, a correlation was found among the *Ins* modeled component of AOD@500 and both OC ($R^2 = 0.5$) and EC ($R^2 = 0.6$) probably because the modeled

Ins component partly accounts for the organic insoluble fraction contribution. This aspect still needs further analysis.

Going to the dust fraction, a comparison was made among the different modeled dust components of AOD@500 and the linear combination of the major terrigenous elements concentrations measured at ground, namely MD_ground ($MD_ground = 2.2*Al + 2.49*Si + 1.63*Ca + 1.94*Ti + 2.42*Fe$). The modeled *MT* component of AOD@500 revealed the best correlation ($R^2 = 0.5$) for the considered days: the corresponding temporal trends are shown in Figure 4.

The great increase of dust component on November 3rd is highlighted both at ground and over the column confirming the changes in aerosol loading at the site.

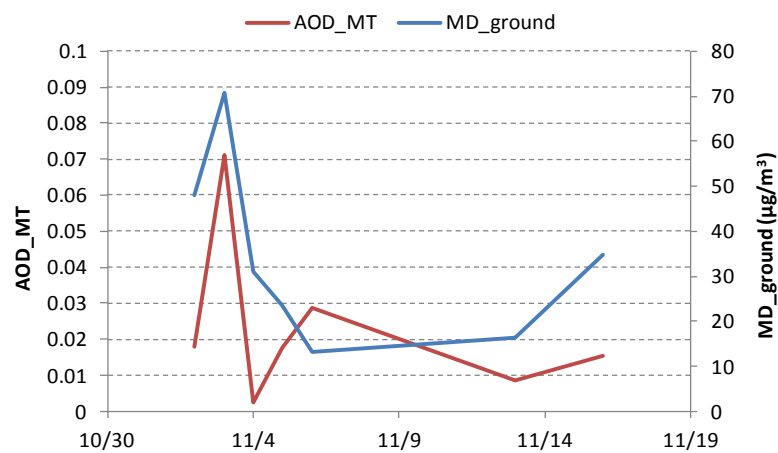


Figure 4. Temporal trends of daily mean *MT* modeled component of AOD@500 and mineral dust fraction measured at ground for 2-6 and 13, 16 November 2012.

3.2 Background days

In order to obtain a more comprehensive description of columnar aerosol characteristics over the urban site of Xi'an, the model was applied to some “background days” chosen among a dataset of Cimel measurements available for 2013 as reported in Table 3.

The criteria used for the data selection were: values of AOD@500 < 0.3/0.5, alpha values ~ 1, a significant number of measurements during the day, seasonal representativeness, availability of simultaneous chemical measurements.

Table 3. Cimel measurements days, number of measurements per day, daily mean AOD@500 and alpha values with corresponding standard deviations for the chosen background days in 2013.

| | Number of measurements | AOD @500 Daily mean \pm St.Dev | Alpha Daily mean \pm St.Dev |
|-------------------|------------------------|-------------------------------------|----------------------------------|
| 24 Jan 13 | 45 | 0.20 \pm 0.03 | 0.81 \pm 0.04 |
| 26 Jan 13 | 34 | 0.36 \pm 0.04 | 0.98 \pm 0.06 |
| 6 Apr 13 | 45 | 0.44 \pm 0.04 | 0.55 \pm 0.09 |
| 11 June 13 | 49 | 0.24 \pm 0.04 | 1.16 \pm 0.07 |
| 12 June 13 | 49 | 0.34 \pm 0.07 | 1.08 \pm 0.09 |
| 30 July 13 | 38 | 0.5 \pm 0.1 | 1.0 \pm 0.1 |

The model was run using the nine components of Table 1 and the corresponding daily mean values are reported in Figure 5.

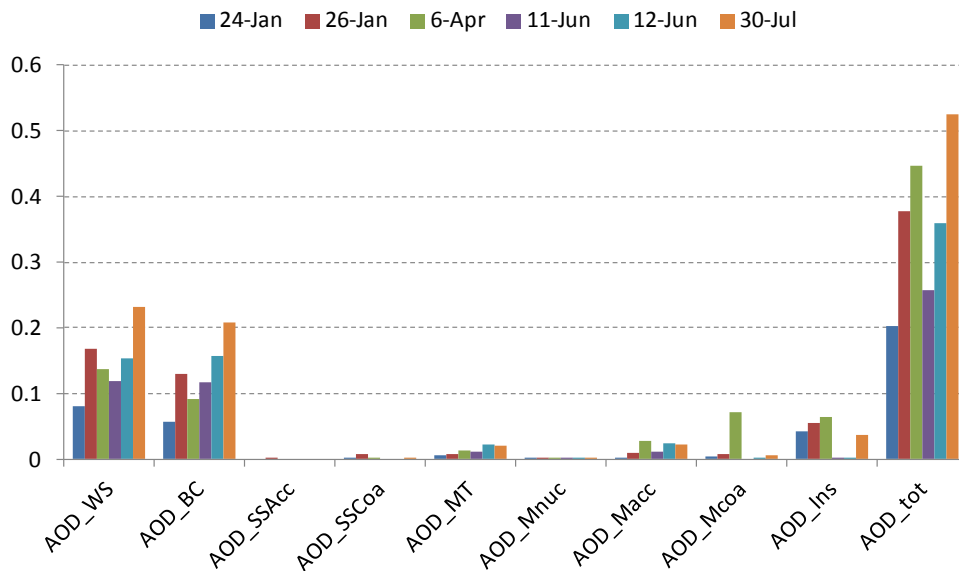


Figure 5. Daily mean values of the model-estimated AOD@500 for each component together with total AOD@500 for the background days (Table 3).

The main modeled components of AOD@500 for background days were *WS* and *BC* indicating that, despite the season, fine particles optical properties dominate over the atmospheric column as expected in such a polluted city. The *Ins* fraction is the third component absent only in June

measurement days. For what concerns the dust components, the two recurrent modes were the *MT* and *Macc* as already found for November 2012, while the *Mcoa* was absent for June measurements and more abundant on April 6th that is the day characterized by the lowest alpha values (Table 3). The *Mnucl*, *SSacc* and *SScoa* components gave a negligible contribution to the total AOD@500 in the case of background days indicating that these components are not locally produced but more probably related to transport phenomena as seen in the previous section for November 3rd 2012. Daily mean percentage contributions are reported in Figure 6 (for the sake of clarity only percentages $\geq 1\%$ were plotted). *WS* and *BC* components accounted for a minimum of 51% on April 6th, to a maximum of 91% on June 11th. *Ins* component was found more abundant in winter (15 and 21%) and early spring (23 %) measurements supporting the hypothesized link with the organic carbonaceous fraction emitted by residential heating during the cold season. If one considers the sum of the three dust components, a percentage contribution varying from 5 % on July 30th to 25% on April 6th was obtained.

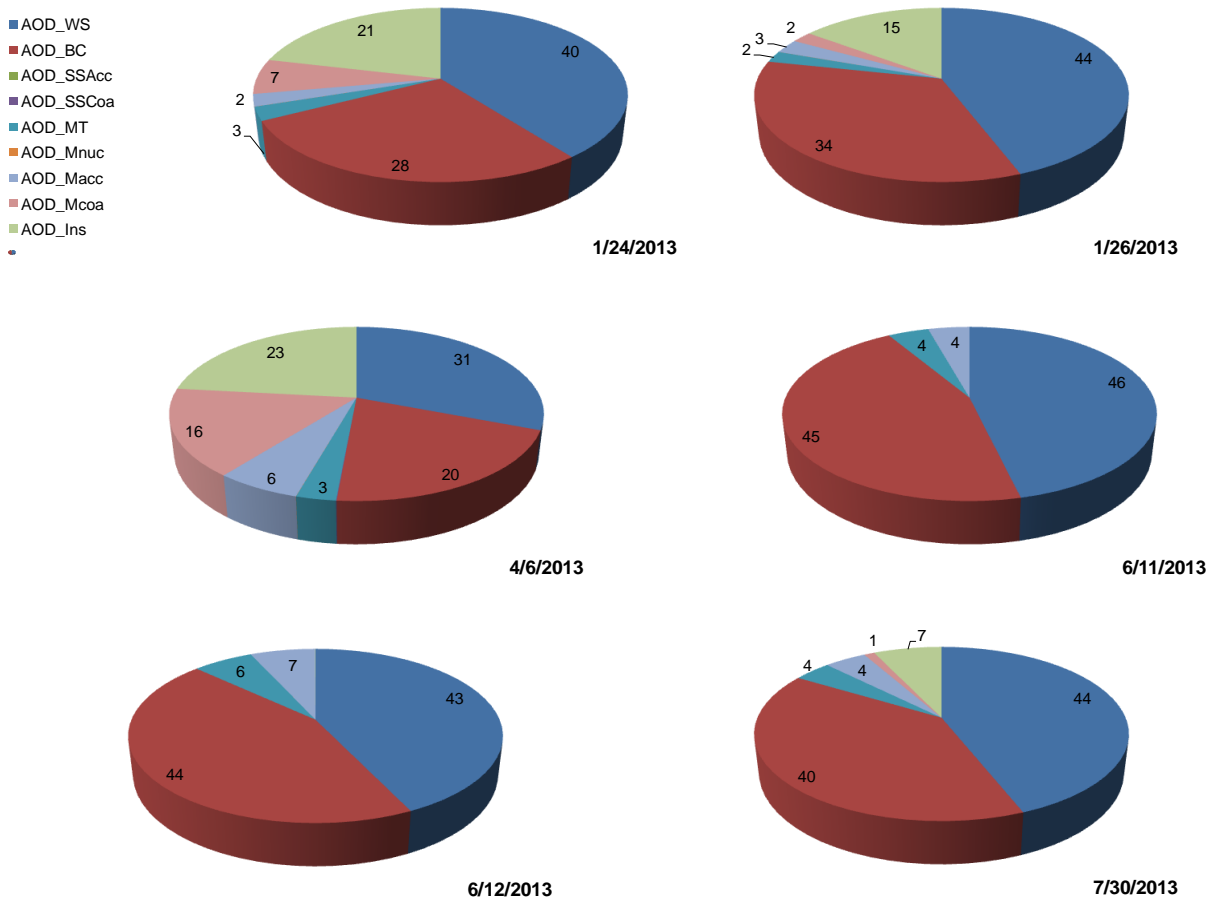


Figure 6. Percentage contributions of the different components to the total AOD@500 for the background days (Table 3).

To complete the description, a comparison was made with in-situ chemical data. A quite good agreement was found again when comparing the modeled *WS* component of AOD@500 and the water soluble fraction measured at ground as shown in Figure 7a confirming that this component strongly influence columnar optical aerosol properties at the site. Similarly for the November measurements, no agreement was found among modeled *BC* component of AOD@500 and both EC and OC concentrations measured at ground probably due to the same reasons explained above, even if further investigations are needed to clarify this aspect.

An interesting finding was that, if the day with the heaviest dust loading (April 6th) was excluded, a correlation coefficient of $R^2 = 0.97$ was found when comparing modeled *Ins* component and EC concentration measured at the ground and of $R^2 = 0.83$ when modeled *Ins* component was compared to OC concentration measured at ground. Lightly lower R^2 values ($R^2 = 0.8$ and $R^2 = 0.7$, respectively) were found if the entire dataset was considered (November measurements days and background days) excluding the two days of high dust loading (November 3rd 2012 and April 6th 2013). This finding confirms the relevant role of this component to the columnar AODs.

Among the modeled dust components, *Mcoa* showed the best correlation with MD_ground ($R^2 = 0.9$) for background days: the corresponding temporal trends are reported in Figure 7b.

If the comparison is extended to the entire dataset, a correlation coefficient of $R^2 = 0.6$ was obtained among the sum of the two modeled components MT and Mcoa and MD_ground suggesting that these two modes can represent dust particles present at the site.

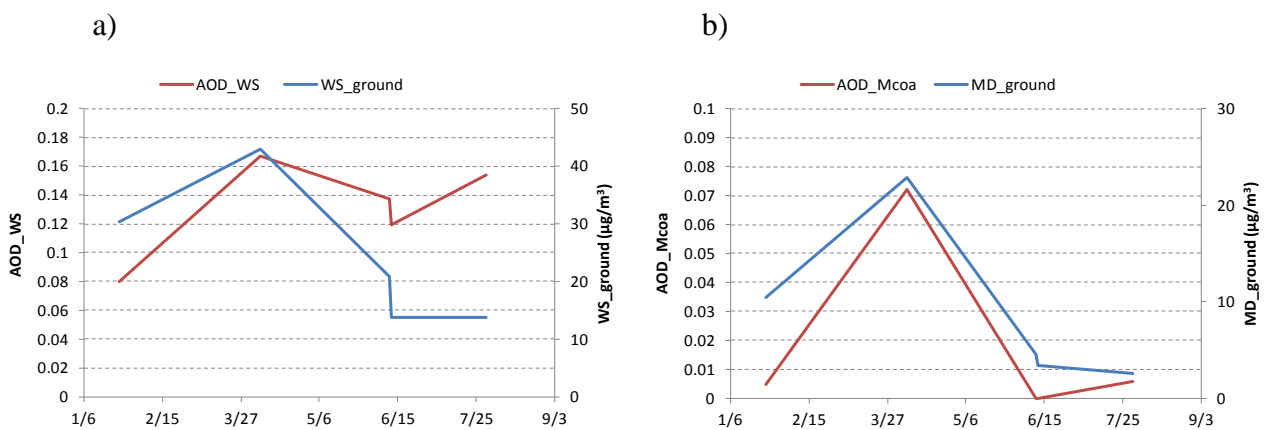


Figure 7. (a) Temporal trends of daily mean *WS* modeled component of AOD@500 and water soluble fraction measured at the ground for background days (Table 3). (b) Temporal trends of daily mean *Mcoa* modeled component of AOD@500 and mineral dust fraction measured at ground for background days (Table 3).

4. Conclusions and future developments

The research activities carried out in the framework of the present STM program represented a successful way to improve the radiometric model performance thanks to the tests carried out for such a complex site. At the same time relevant information on aerosol columnar composition at Xi'an urban site were obtained for the first time. The comparison among model results and in-situ chemical data helped to understand how ground level aerosol properties are related to columnar ones. Although preliminary, the obtained results represent a stimulus to continue the study, going ahead with the collaboration with colleagues at IECAAS, also planning to submit joint papers to International journals.

In addition, the favourable synergy established with the research group at IEECAS during the STM strengthened the will to work together to submit joint proposal for international projects.

Acknowledgements

I would like to thank:

- CNR, for the financial support in the framework of the STM program 2015;
- IEECAS for the kind hospitality, the facilities and the data made available;
- Prof. Junjii Cao and Prof. Xiaoli Su for the kind hospitality and the scientific support.

References

- van Beelen, A. J., Roelofs, G. J. H., Hasekamp, O. P., Henzing, J. S., Röckmann, T. Estimation of aerosol water and chemical composition from AERONET Sun-sky radiometer measurements at Cabauw, the Netherlands. *Atmos. Chem. Phys.*, 14, 5969–5987. (2014).
- Calvello, M., Esposito, F., Pavese, G., Serio, C. Physical and optical properties of atmospheric aerosol by in-situ and radiometric measurements. *Atmos. Chem. Phys.* 10, 2195-2208. (2010).
- Cao, J. J., Wu, F., Chow, J. C., Lee, S. C., Li, Y., Chen, S. W., An, Z. S., Fung, K. K., Watson, J. G., Zhu, C. S., and Liu, S. X. Characterization and source apportionment of atmospheric organic and elemental carbon during fall and winter of 2003 in Xi'an, China. *Atmos. Chem. Phys.*, 5, 3127–3137. (2005).
- Cao, J. J., Lee, S. C., Chow, J. C., Watson, J. G., Ho, K. F., Zhang, R. J., Jin, Z. D., Shen, Z. X., Chen, G. C., Kang, Y. M., Zou, S. C., Zhang, L. Z., Qi, S. H., Dai, M. H., Cheng, Y., and K. Hu. Spatial and seasonal distributions of carbonaceous aerosols over China. *Journal of geophysical research*, vol. 112, D22S11, doi:10.1029/2006JD008205. (2007).

- Cao, J. J., Zhu, C. S., Chow, J. C., Watson, J. G., Han, Y., Wang, G., Shen, Z., An, Z. Black carbon relationships with emissions and meteorology in Xi'an, China. *Atmospheric Research* 94, 194–202. (2009).
- Cao, J. J., Zhu, C., Hoc, K., Hana, Y., Shen, Z., Zhan, C., Zhang, J. Light attenuation cross-section of black carbon in an urban atmosphere in northern China. *Particuology*, 18, 89–95. (2015).
- Cui, H., Mao, P., Zhao, Y., Nielsen, C. P., and Zhang, J. Patterns in atmospheric carbonaceous aerosols in China: emission estimates and observed concentrations. *Atmos. Chem. Phys.*, 15, 8657–8678. (2015).
- Esposito, F., Calvello, M., Pavese, G. Abstract of the PM 2014. (2014).
- Hess, M., Koepke, P., and Schult, I. Optical Properties of Aerosols and Clouds: The Software Package OPAC. *Bull. Amer. Meteor. Soc.*, 79, 831–844. (1998).
- Hu, T., Cao, J., Shen, Z., Wang, G., Lee, S., Ho, K. Size Differentiation of Individual Atmospheric Aerosol during Winter in Xi'an, China. *Aerosol and Air Quality Research*, 12: 951–960. (2012).
- Huang, R., Zhang, Y., Bozzetti, C., Ho, K., Cao, J., Han, Y., Daellenbach, K. R., Slowik, J. G., Platt, S. M., Canonaco, F., Zotter, P., Wolf, R., Pieber, S. M., Bruns, E. A., Crippa, M., Ciarelli, G., Piazzalunga, A., Schwikowski, M., Abbaszade, G., Schnelle-Kreis, J., Zimmermann, R., An, Z., Szidat, S., Baltensperger, U., El Haddad, I., & Prevot, A.S. H. High secondary aerosol contribution to particulate pollution during haze events in China. *Nature*, 514, doi:10.1038/nature13774. (2014).
- Latha, R., Murthy, B.S., Manoj Kumar, Jyotsna, S., Lipi, K., Pandithurai, G., Mahanti, N.C. Aerosol Optical Properties and Composition over a Table Top Complex Mining Area in a Monsoon Trough Region. *Aerosol Air Qual. Res.*, 14, 806–817. (2014).
- Pavese, G., Lettino, A., Calvello, M., Esposito, F., Fiore, S. An integrated approach to characterize long-range transported dust. *ProScience* 1, 186-191; DOI:10.14644/dust.2014.030186-191. (2014).
- Perrone, M. R., Romano, S., Orza, J. A. G. Columnar and ground-level aerosol optical properties: sensitivity to the transboundary pollution, daily and weekly patterns, and relationships. *Environ. Sci. Pollut. Res.*, DOI 10.1007/s11356-015-4850-7. (2015)
- Rohde R. A., Muller R. A. Air Pollution in China: Mapping of Concentrations and Sources. *PLoS ONE* 10(8): e0135749. doi:10.1371/journal.pone.0135749. (2015).
- Satheesh, S. K., and Srinivasan, J. A Method to Estimate Aerosol Radiative Forcing from Spectral Optical Depths. *J. Atmos. Sci.*, 1082-1092, 63. (2005).
- Shen, Z., Cao, J., Liu, S., Zhu, C., Wang, X., Zhang, T., Xu, H., & Hu, T. Chemical Composition of PM₁₀ and PM_{2.5} Collected at Ground Level and 100 Meters during a Strong Winter-Time Pollution Episode in Xi'an, China. *J. Air & Waste Manage. Assoc.* 61:1150–1159. (2011).
- Shon, Z., Ghosh, S., Kim, K., Song, S., Jung, K., Kim, N. Analysis of water-soluble ions and their precursor gases over diurnal cycle. *Atmospheric Research* 132–133, 309–321. (2013).

Sinha, P. R., Manchanda, R. K., Kaskaoutis, D. G., Kumar, Y. B., Sreenivasan, S. Seasonal variation of surface and vertical profile of aerosol properties over a tropical urban station Hyderabad, India. *J. Geophys. Res.*, 118, 749–768. (2013)

Su, X., Cao, J., Li, Z., Lin, M., Wang, G. Column-Integrated Aerosol Optical Properties during Summer and Autumn of 2012 in Xi'an, China. *Aerosol and Air Quality Research*, 14: 850–861. (2014).

Zhang, T., Cao, J.J., Tie, X. X., Shen, Z. X., Liu, S. X., Ding, H., Han, Y. M., Wang, G. H., Ho, K. F., Qiang, J., Li, W. T. Water-soluble ions in atmospheric aerosols measured in Xi'an, China: Seasonal variations and sources. *Atmospheric Research* 102, 110–119. (2011).